Hybrid nanomaterials based on gum Arabic and magnetite for hyperthermia treatments

M. Fernanda Horst [a,*], Diego F. Coral [b], Marcela B. Fernández van Raap [b], Mariana Alvarez [a], Verónica Lassalle [a]

[a] INQUISUR-CONICET, Dto. Química, Universidad Nacional del Sur, Bahía Blanca, Buenos Aires, Argentina
[b] Instituto de Física La Plata IFLP-CONICET, Departamento de Física, Universidad Nacional de La Plata, La Plata, Buenos Aires, Argentina

ABSTRACT

In this study, one–step co-precipitation method was conveniently adapted to obtain novel nanomaterials based on Gum Arabic and magnetite. Two synthesis procedures were evaluated: one employing the solid biopolymer in the co-precipitation media; a second using an aqueous solution of the polysaccharide. An exhaustive characterization of both formulations was performed using several specific techniques. The obtained data confirmed the successful incorporation of the gum Arabic on the magnetic core. Values of hydrodynamic diameters, measured by dynamic light scattering, in aqueous dispersions were about 70–80 nm, while sizes lower than 20 nm were registered by TEM microscopy. Surface charge of gum Arabic coated magnetic nanoparticles was significantly different from the corresponding to raw materials (magnetite and GA). This fact confirmed the formation of hybrid nanosystems with novel and specific properties.

The potential utility of these materials was tested regarding to magnetic hyperthermia therapy under radiofrequency fields. Magnetocalorimetric measurements were performed in a wide range of field amplitude and frequency. Specific absorption rate of 218 W/gFe was determined at field frequency of 260 kHz and amplitude of 52 kA/m. These results demonstrate their viability to be applied in tumor ablation treatments. Using the linear response theory and restricting field parameters to the accepted biomedical window, maximum useful value of 74 w/gFe is predicted at 417 kHz and 12 kA/m.

© 2016 Elsevier B.V. All rights reserved.

1. Introduction

The fabrication of hybrid polymeric/magnetite materials originates a novel kind of tools able to solve problems in several fields such as environmental remediation, biomedicine, electronic, etc. The impact of these materials in the mentioned areas is related to their specific properties, which are largely different from the expected for each component separately [1–5].

Among the available literature, general approaches commonly described to prepare polymeric coated magnetic nanoparticles (MNPs) are based on simple co-precipitation method [6]. In this context two main alternatives may be found in terms of the polymer addition. The first one consists in dissolving both, precursors of iron oxide and the polymer in the same reaction media. The aim is promoting a control of size and morphology of the magnetic nucleus by means of the polymeric matrix [7,8]. The other method involves the polymer incorporation on magnetic cores previously synthesized. Those procedures comprise the direct grafting [9], ligand exchange [10] or hydrophobic interactions

[11]. Biopolymers including agarose, alginate, carrageenan, chitosan and dextran, have been widely employed to these ends. Among others such as gum Arabic, pullulan and starch that have been less explored [4].

Gum Arabic (GA) is especially attractive as magnetite nanoparticles coating because of its stabilizer, hydrocolloid emulsifier and biocompatibility properties. GA consists of three fractions with distinct chemical structures where the major one is a highly branched polysaccharide with a molecular weight of about 3×10^5 g/mol [12].

After a survey of available literature it was found that the articles reporting the use of this biopolymer as coating of magnetic nanoparticles are very limited [13–22]. For example, Banerjee et al. synthetized GA-magnetic nanoparticles obtaining firstly the magnetic cores and then coating with GA [15]. In this work, specific linkers were incorporated to the synthesis pathway aiming to attach glucose and cyclodextrins to the GA-magnetic nanoparticles, as a way to increase their functionality.

Meanwhile, Roque et al. [14] prepared MNPs coated with GA via adsorption and covalent coupling, and compared their characteristics as a function of the synthesis method. The authors employed glutaraldehyde and *N*-(3-dimethylaminopropyl)-*N*′-ethylcarbodiimide to provide amine groups to magnetic nanoparticles that were then utilized to attach biomolecules such as proteins.

* Corresponding author at: INQUISUR-CONICET-UNS, Av. Alem 1253, B8000CPB Bahía Blanca, Argentina.
E-mail address: mfhorst@uns.edu.ar (M.F. Horst).

In another work, MNPs were synthesized under acidic conditions in presence of oleylamine and GA to evaluate the influence of surface modification on MNP characteristics and cellular level bioactivity. These authors found that MNPs coated with GA formed large particle aggregates that exhibited rapid coagulation [13].

The application of magnetic nanoparticles to the healthy is an increasingly common practice that is being implemented for several purposes. Between the available raw materials, magnetite in the nanoscale is the preferred; in fact NPs based on iron oxide (Fe_3O_4) was approved for medical uses by the USA Food and Drug Administration (FDA) and the European Medicines Agency (EMA) [23].

In particular, their use in tumor therapies, as target drug delivery devices or for hyperthermia, has been widely explored in the last decades [24].

Hyperthermia is one of the powerful techniques for treatment of cancer diseases. This therapeutic procedure consists of rising the temperature of living cells above the physiological levels, at values around 42–43 °C using an AC magnetic field. On this way, the damage is restricted to cancer cells in a very short time avoiding the toxic effect in surrounding cells and tissues [25].

In this context it is clear that the properties of the magnetic nanoparticles are a key factor in determining the successful of hyperthermia treatments. The selection of a suitable coating is strongly required in order to achieve adequate biodegradability and biocompatibility, whereas conveniently adjusting size and dispersion ensures superparamagnetism property [7,26,27].

This work deals with the preparation of magnetic nanoparticles employing a non-well explored polysaccharide such as gum Arabic as stabilizer of iron oxide core. The aim is to obtain biocompatible nanodevices with potential in hyperthermia treatments.

To this end, magnetic nanoparticles were obtained by a non-time consuming and low cost method based on the traditional in situ co-precipitation. In this case, variables associated to the synthesis procedure were analyzed aiming to reach the optimum methodology regarding the magnetic nanoparticles properties, mainly size, surface charge and stability.

The proposed synthesis involved a unique step were the formation of magnetic cores and GA coating occurred simultaneously. This fact may be considered as the mayor difference regarding to the available information about MNPs-GA preparation.

The performance of MNPs-GA aqueous suspensions was assayed in terms of their response to magnetic hyperthermia. Although this application is well established employing a wide gamma of magnetite nanoparticles [28], the use of MNPs-GA for magnetic hyperthermia has not been earlier reported to the best of these author's knowledge [29]. Viability studies in HCT116 cell line (human colon carcinoma) incubated with several Fe/GA-MNPs ratios have shown the potentiality of a similar formulation for biomedical applications [30].

2. Experimental

2.1. Materials

GA was provided by *Biopack* (*Argentina*). Iron(II) sulfate, heptahydrated, and iron(III) chloride, hexahydrated, were purchased from Cicarelli Laboratory (Argentina), hydrochloric acid was from Biopack (Argentina) and ammonium hydroxide was provided by Anedra Laboratory (Argentina). Analytical grade solvents and other reactants were employed.

2.2. Methods

2.2.1. Synthesis of magnetic nanoparticles

The magnetic nanoparticles were synthesized by an adaptation of co-precipitation method earlier reported [8]. Conventionally, magnetite is prepared by the addition of a base to an aqueous mixture of Fe^{+2} and Fe^{+3} salts whose molar ratio is commonly 1:2, under inert atmosphere at moderate temperatures (between 50 and 80 °C). In this case, 3.254 g $FeCl_3 \cdot 6H_2O$ (0.0125 mol de Fe^{3+}) and 1.789 g $FeSO_4 \cdot 7H_2O$ (0.00625 mol de Fe^{2+}) were dissolved in 100 mL of distilled water. Then, two alternatives for biopolymer incorporation were evaluated: a) addition of solid GA (1 g) to the iron solution, and b) addition of 10 mL of 10% w/w GA solution. The suspensions were stirred at 70 °C during 30 min under N_2 bubbling. Then, 17.56 mL of NH_4OH 5 M were added to induce formation of magnetic particles. The obtained materials were washed several times with distilled water. The solid product was separated by magnetic decantation, dried at 45 °C and gently crushed. Magnetic nanoparticles arising from each synthesis procedure were named as GA-Mag-a (where GA was added in solid state) and GA-Mag-b (where GA was added as solution), respectively. Fig. 1 shows a photograph of raw gum Arabic and GA-Mag-a, as example. This fact could be considered as a first proof of the formation of new materials with specific characteristics. The obtained magnetic materials were used as solid or suspension due to the assay to be performed. Solid nanoparticles were separated by magnetic decantation, dried at 45 °C and gently crushed, and another portion of MNPs were left in aqueous suspensions.

2.2.2. Characterization

The MNPs-GA as well as raw materials, were characterized by FTIR to corroborate the presence of polymeric and magnetic moieties. A FTIR (DRIFTS) Thermo Scientific Nicolet 6700 spectrometer was used for recording spectra in the range 4000–400 cm^{-1}. Composition of magnetic materials in terms of Fe content was determined using atomic absorption GBC Avanta 932 Spectrometer. Meanwhile solid concentration in aqueous magnetic suspensions was determined by gravimetric measurements. The estimated concentration was 4.57 mg magnetic nanoparticles per mL of suspension.

The nanomaterials morphology was observed by transmission electron microscopy (TEM) using a microscopy JEOL 100 CX II, JEOL, Tokyo, Japan (1983).

X-ray diffraction (XRD) patterns were analyzed to identify crystalline phases of the obtained iron oxide. The assays were recorded by a PHILIPS PW1710 diffraction spectrometer with anode of Cu and curve graphite monochromatic.

Average hydrodynamic particle diameters (Dh) were determined by dynamic light scattering (DLS) using a Malvern Zetasizer equipment. The same equipment was also employed to measure the Z potential (ξ) of magnetic nanoparticles and raw materials. This parameter was measured in the range of pH 3.0–9.0 to determine the pH at point zero charge (pH_{zc}), which was defined as the pH value where ξ is equal zero. 5 mg of dried nanoparticles was added to 100 mL of a 1×10^{-2} M KNO_3 solution obtaining a solid/solution ratio of 20. The pH was adjusted by adding 0.1 M of KOH or HNO_3. The electrophoresis cell was washed and rinsed several times with distilled water before measurements to avoid cross-contamination. Three replicates were performed with each sample.

Specific magnetization (M) as a function of applied magnetic field (H) at room temperature was obtained using vibrating sample magnetometer (VSM) LakeShore 7404 operated with maximum applied fields $\mu_0 H_{max} = 1.8$ T. For measurements, 50 μL of colloidal suspension were sealed into a heat shrinkable tube to prevent samples evaporation and spills.

Thermogravimetric analyses (TG) were performed using Rigaku DTA-TAS 1000 equipment. Different masses of magnetic nanoparticles, magnetite and GA were weighted and heated from room temperature to 500 °C. The air flow rate was fixed of 10 °C/min.

2.2.3. Stability

The evolution of the hydrodynamic diameter as a function of the time was considered as a measurement of the nanoparticles stability. To achieve these data, 1 mg of GA-magnetic nanoparticles was
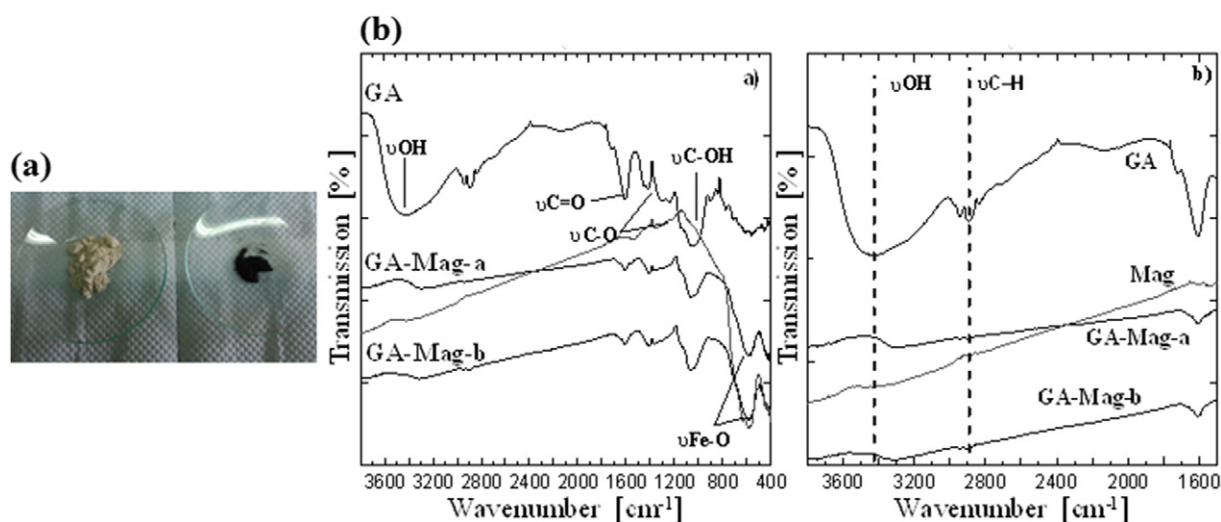
Fig. 1. a). Photograph of raw Arabic gum (left) and dry GA-Mag nanoparticles (right) b). FTIR spectra of Arabic gum, GA-Mag nanoparticles and Fe_3O_4 (grey line).

dispersed in aqueous media and ultrasonicated during 1 h. The measurements were periodically repeated along the time.

The same procedure was reproduced but using a mixture of ethanol/water (1/1) as dispersant media.

2.2.4. Magneto calorimetric assays

Time-dependent calorimetric experiments for determining Specific Adsorption Rate (SAR) were conducted by exposing 0.5 mL of the aqueous suspension, hold in a clear glass Dewar, to 260 kHz and field amplitude varying in the range from 2 to 52 kA/m. In a second experiment, field amplitude was hold at 17.4 kA/m while frequency was varied between 70 and 260 kHz. Field generator consist of a resonant RLC circuit Hüttinger (2.5/300) with a water refrigerated 5 turns coil of 2.5 cm diameter. The temperature was sensed during the experiment with an optical fiber sensor placed in the sample centre. The sensor was connected to a calibrated signal conditioner (Neoptix) of an accuracy of ± 0.1 °C. Colloid temperature was kept below 30 °C in order to minimize solvent evaporation and prevent its destabilization.

The SAR values were calculated from the initial slope $\partial T/\partial t$ of experimental heating curves as $SAR = \frac{C}{[x]}\frac{\partial T}{\partial t}$ where C is the volumetric heat capacity of the solvent 4.18 J/cm^3 K and $[x]$ is the MNP concentration in the colloid.

3. Results and discussion

3.1. Characterization of the magnetic nanoparticles

3.1.1. FTIR-DRIFTS

FTIR technique was employed to investigate the binding of gum Arabic to magnetite. Fig. 1b displays the spectra of magnetic nanoparticles, and raw materials. The spectrum of biopolymer exhibits bands at 1050 cm^{-1}, due to stretching of C—O (C—OH), at 1425 and 1275 cm^{-1}, assigned to torsion/stretching of hydroxylic group, and at 1612 cm^{-1} corresponding to C=O. Signals associated to υCH_3 y CH_2 appear at 2887 y 2950 cm^{-1}; while bands at 3000–3600 cm^{-1} could be attributed to O—H stretching. Although the presence of amine groups in gum Arabic has been recognized [31], independent bands arising from these functional groups are not distinguished belcause they overlap with the broad absorption signal at ~3500 cm^{-1} due to O—H from polysaccharide. Similar results were achieved by Banerjee and Chen [15]. Magnetite spectrum exhibits bands in the range of 1000–500 cm^{-1} due to the iron oxide skeleton. A strong band near 570 cm^{-1} appears, and is typical of Fe—O bond [32]. The characteristic bands of gum Arabic together with an intense absorption band at ~600 cm^{-1} are observed in

the spectra of both magnetic nanoparticles. The latter reveals the effective binding of biopolymer onto the magnetite, independent on the synthesis pathway.

Furthermore, a slight shift of the signal ascribed to O—H stretch, at 3450 cm^{-1}, is noted in the spectra of magnetic nanoparticles when comparing with the GA spectrum. These evidences could be associated to the occurrence of hydrogen bridge interactions between carboxylic groups of GA and the surface hydroxyl groups of Fe_3O_4 particles. Similar findings were achieved by other authors studying analogous inorganic-GA systems [15,20].

3.1.2. Composition of GA-Mag

The magnetite content in the nanoparticles was determined by atomic absorption in terms of the amount of Fe and it was expressed as % Fe_3O_4. The calculated magnetite percentage was 43.3 and 53.8 for GA-Mag-a and GA-Mag-b, respectively. This may us infer that the magnetic phase have almost the same proportion in both materials, independently on the synthesis route. These results agree with the nominal amount of biopolymer and magnetite used during the synthesis (see Section 2.2.1). Besides, this data is consistent with our previous research involving other magnetic systems obtained through the same methodology [8].

3.1.3. XRD patterns

X-ray diffraction was used to identify the crystalline pattern of the iron oxide in nanoparticles. Fig. 2 compares the patterns of both magnetic materials highlighting the crystallographic reflexion lines of spinel structure consistent with cubic spinel structure (space group Fd3m) attributable to crystalline structure of magnetite and/or maghemite. The presence of spinel phase of these iron oxides is clearly evidenced in both difractograms. It is worth noting that the crystalline structure of Fe_3O_4 remains unaffected by the presence of the biopolymeric moieties, even when it was incorporated at very early stages during co-precipitation. These results agree with those reported by other authors working with similar magnetic systems [18,20]. The XRD patterns for GA-MNPs, in the mentioned researches showed identical indices (hkl); (220), (311), (400), (422), (511), and (440). The XRD analysis of pure GA confirmed the amorphous nature of the polymer, and was in accordance with information of available literature [33]. Therefore, as expected, the crystallinity of the nanoparticles may be exclusively ascribed to the iron oxide component.

3.1.4. Thermogravimetric analysis

Thermogravimetric analyses were conducted to estimate the MNPs composition, in terms of the amount of gum Arabic attached onto the
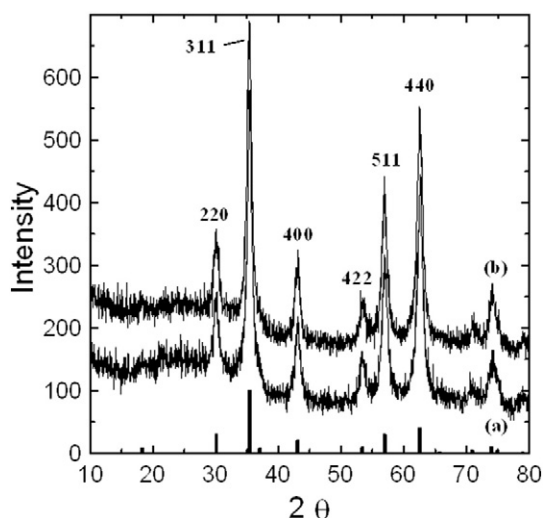
Fig. 2. XRD pattern of GA-Mag-a (a), GA-Mag-b (b). Crystallographic pattern of Fe_3O_4 is indicated in plot.

Fe_3O_4 surface and also to identify the degradation temperature of magnetic nanoparticles. Fig. 3 shows the curves expressed as % of lost mass (w/w) as a function of the temperature in the range from 30° to 500 °C. The only weight loss observed in raw Fe_3O_4 thermogram is about 5%. This is attributed to residual surface and interstitial water content. Meanwhile, GA thermogram exhibits two weight loss steps. The first one, occurs from 25° to 137 °C range approximately, may be associated to loss of residual water in the biopolymer. The second, in the region of 225°–375 °C may be associated to decomposition, depolimerization and scission of carboxylate groups from polymeric chains [34]. It is worth noting that both materials display two weight loss steps in their thermograms. The first, over 25° to 135 °C, may be assigned to the weight loss of residual water in the surface of the GA -MNPs. The second step attributable to decomposition of GA is observed from 150° to 350 °C. From the obtained data, it is noted that GA-Mag-a undergoes a total weight loss of ~39%; while GA-Mag-b presents a final weight loss of around 22%. Although the nominal amount of gum Arabic was the same in both magnetic nanoparticles formulations, these results indicate a higher GA incorporation when it was added in solid state in the co-precipitation media. The lower proportion of GA incorporated in GA-Mag-b could be due to the loss of low M_w GA fractions during the dissolution process. Similar results were obtained by Williams et al. in
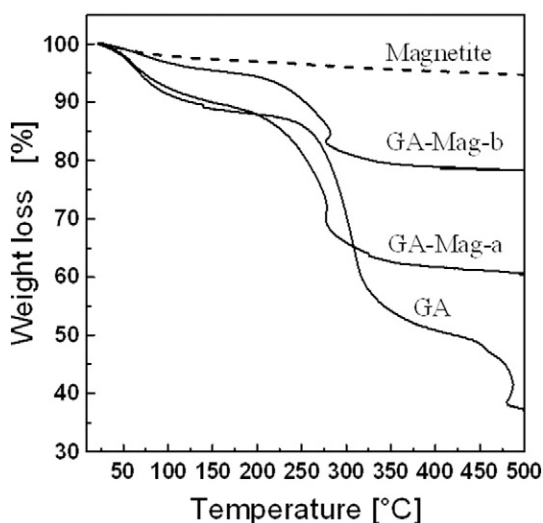
GA-coated magnetite and magnetite co-precipitated with the same polymer. These authors attributed differences observed to stronger physical adsorption of GA onto the surface of magnetite particles. They postulated that the glycoprotein fraction in GA was responsible of binding interactions that appear in the initial stages, between functional groups of GA (NH, OH, CO) and the nucleus in formation of magnetite [16].

3.1.5. TEM and dynamic light scattering

The average diameters measured in ethanol/water and in water; are listed in Table 1. The Dh of both formulations was comprised between 500 and 700 nm when the measurement was conducted on ethanol/water media. It is noteworthy that the average size of naked Fe_3O_4 in the same media was around 400 nm. The Dh of the polymer could not be measured due to the formation of aggregates of too large sizes [8]. Lower Dhs values were recorded using distilled water as dispersant, as it is appreciated in the Table.

It is important to note that the registered Dhs (in both media) resulted lower than some data reported regarding to similar systems prepared by alike procedures. For instance, Wilson et al. [13] informed a hydrodynamic diameter of about 1 μm for composites obtained by adding GA during magnetite precipitation. These authors also synthesized the GA-modified magnetic particles by incorporating the polymer in solid state to a given volume of iron ion solutions, prior to the alkali addition.

The analysis achieved by TEM supported the results from DLS; since a similar trend was evidenced by comparing morphology and sizes obtained from GA-Mag dispersed in both media (water and EtOH/water). These findings are depicted in Fig. 4. In the case of Fig. 4a), it is clear that highly aggregated magnetite nanoparticles are dispersed in GA matrix. The sizes estimated of those aggregates are around 400–500 nm. The nanoparticles behavior in water dispersion is fully different, as reveal Fig. 4b). In this case, relatively monodisperse, spherical nanoparticles in shape are observed. Even when aggregates may be present, their sizes - as estimated by TEM - appear to be lower than 50 nm. These results agree with data on Table 1 concerning to Dh values as a function of the dispersant media.

The stabilization mechanism, associated to the surface charge and the interaction way of GA-Mag during the nanoparticles formation, is the responsible of this behavior; as will be later in deep discussed.

3.1.6. ζ Measurements

The surface charge of GA-Mag nanoparticles and raw GA were determined by evaluating ζ as a function of pH. This data is included in Fig. 5. ζ of Mag, GA and GA-Mag nanoparticles increased with the reduction of pH due to the protonation of the hydroxyl groups in the case of magnetite (OH— due to the water adsorption on the iron oxide surface) or the carboxylic groups in the case of the GA. In the GA-Mag nanoparticles, this trend could be related to a combination of both functional groups. As could be seen, pH of GA point zero charge (PZC) was around ~2.55. This could be attributed to the protein fractions in biopolymer. Amino acids like arginine, aspartic and glutamic acids have α-carboxylic groups with pK_a in the range 1.8–2.2 [35]. Similar pH_{PZC} value for GA was

Fig. 3. Weight loss (expressed as %) as function of temperature of raw materials and GA-Mag nanoparticles.

Table 1
Hydrodynamic diameter and polydispersity index of GA and GA-Mag nanoparticles dispersed in ethanol/water and water.

Material	Dh[a] (nm)	Dispersion media	PDI
GA	549.6 ± 9.5		0.773[b]
GA-Mag-a	735.3 ± 11.7	Ethanol/water	0.230
	73 ± 12.85	Water	0.349
GA-Mag-b	535 ± 8.2	Ethanol/water	0.411
	88 ± 14.85	Water	0.370

[a] Data corresponding to Dh expressed in number.
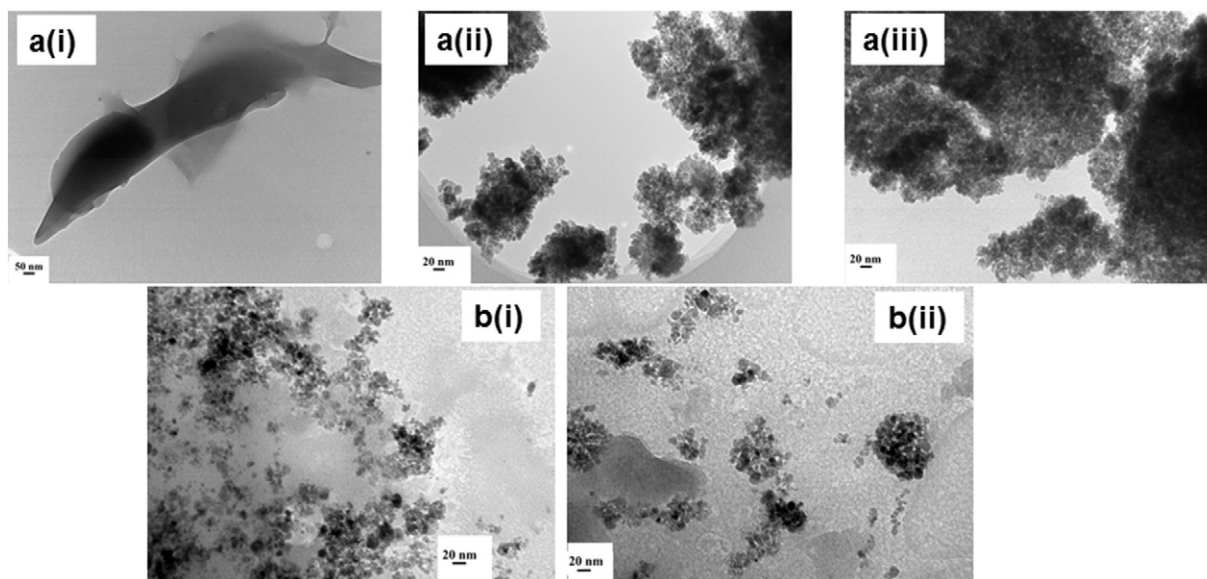[b] Quality criteria of equipment not good.

Fig. 4. Micrographies TEM of Arabic gum and GA-Mag nanoparticles: a) ethanol/water dispersion: (i) GA, (ii) GA-Mag-a and (iii) GA-Mag-b; b) water media: (i) GA-Mag-a, (ii) Ga-Mag-b.

informed by other authors [41]. Meanwhile, the pH_{PZC} for raw Fe_3O_4 was 7.1 and the values corresponding to GA-Mag-a and GA-Mag-b were 3.25 and 2.42, respectively.

The shifts of the pH_{PZC} of the GA-Mag nanoparticles with respect to the corresponding to pure iron oxide suggest that functional groups of different nature are exposed on nanoparticles surface. This is a consequence of the way as GA was bind during the synthesis, as will be later better explained. The obtained results are in accordance with those reported by Wilson et al. working with similar materials. The justification offered by these authors is related to the mechanism of nanocomposites formation in the precipitation media [13].

It is important to highlight that materials prepared by different synthesis pathways do not exhibited important differences in the evolution of Z potential vs. pH, which is a proof that the formation mechanisms are almost similar in both cases.

On the other hand, considering that the pH range associated to main applications of these materials (biomedicine, environmental remediation etc.) is between 5 and 7, it may state that both samples are within the range of electrostatic colloid stability since the ζ is lower than – 15 Mv.
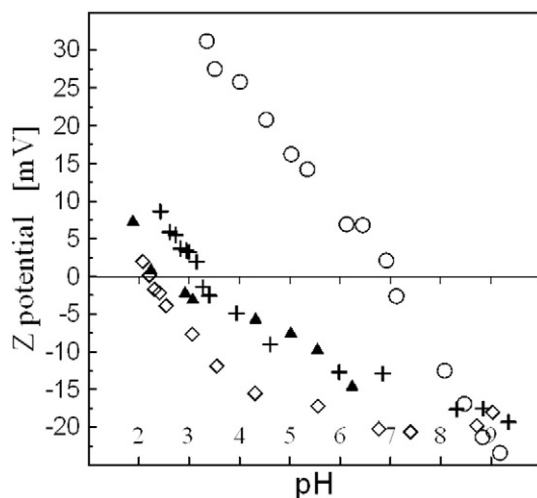
3.1.7. Magnetic properties

Magnetic measurements registered using both materials display a typical superparamagnetic behavior characteristic of single magnetic domain particles. Magnetization of GA-Mag-b also was measured in aqueous suspension at 1.44 mg_{Fe}/ml (Fig. 6). Saturation magnetization of 44.2 emu/g (equivalent to 137.2 emu/g_{Fe}) and mean particle magnetic moment $<\mu> = 15,065$ μ_B were obtained fitting a Langevin function to experimental data, this mean magnetic moment is consistent with size particle around 6.3 nm. *Ms* value obtained for particles in suspension is similar to that obtained for the dried samples.

3.2. Stability assays

The stability of the nanoparticles was firstly evaluated in terms of their ability to form stable dispersions in different media. To do this, 1 mg of solid material was dispersed in 10 mL of ethanol/water solution and water, respectively. The difference in the behavior is shown in Fig. 7(a), where it is clear that a homogeneous colloidal dispersion was achieved in water while large precipitated aggregates were observed in the hydro-alcoholic mixture. This is a consequence of the
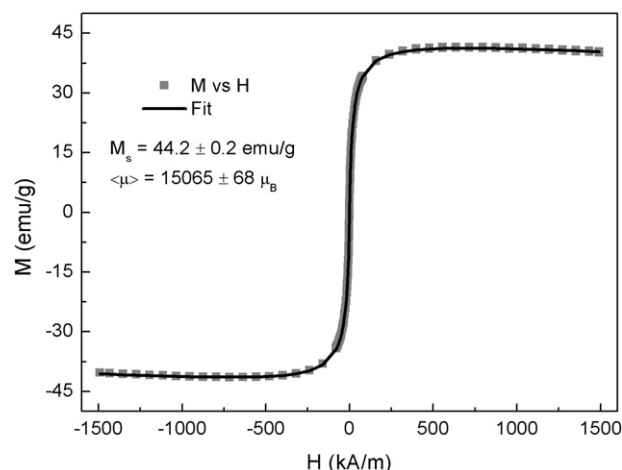

Fig. 5. Z potential as function of pH of: (O) Mag, (▲) GA, (×) GA-Mag-a, (◇) GA-Mag-b.

Fig. 6. Magnetization curves at room temperature of GA-Mag-b nanoparticles.
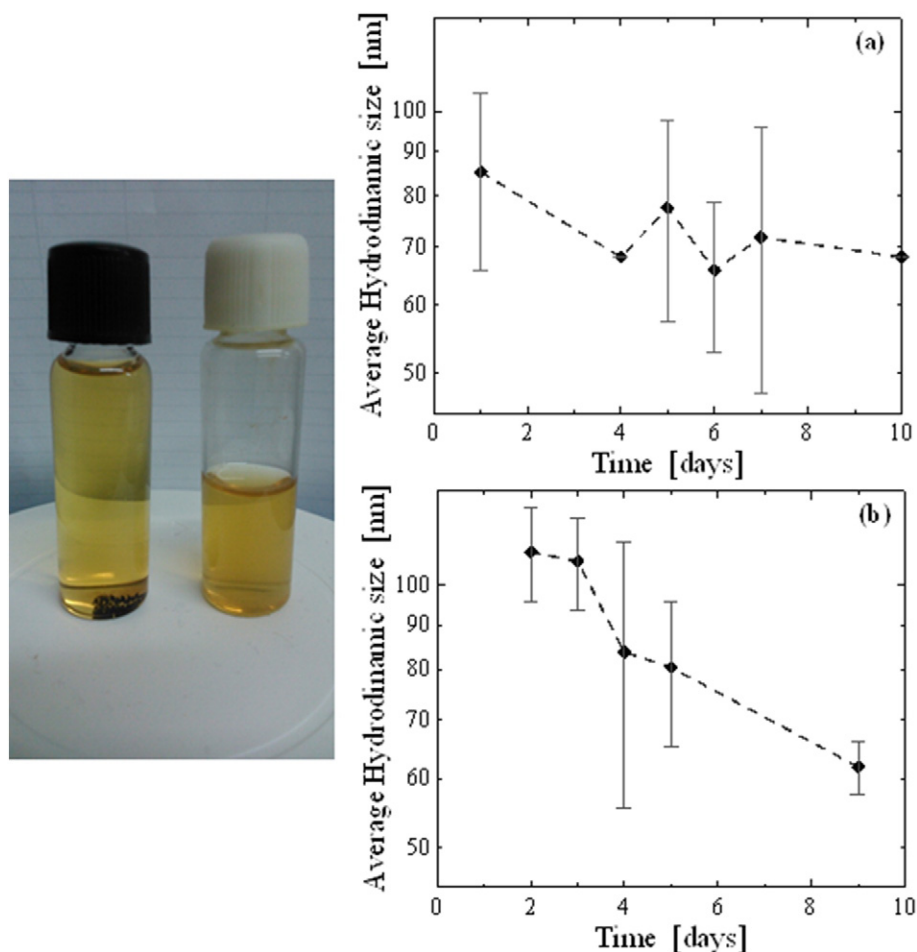
Fig. 7. a). Photographs of GA-Mag nanoparticles dispersed in ethanol/water (left) and water (right); b). Average hydrodynamic size (Dh) in water of: i) GA-Mag-a and ii) GA-Mag-b as a function of time.

mechanism of GA stabilization on the iron oxide, which leads to strongly hydrophilic nanoparticles.

Secondly, the stability of NPs in water dispersions was determined by measuring the evolution of the colloids sizes (as Dh) along the time. Hydrodynamic diameters were recorded during 10 days, and the results are depicted in Fig. 7(b). Regarding GA-Mag-a, the data of Dh vs. time it may infer that, although a slight decrease on hydrodynamic average diameter value was observed along the days, it did not represent a great extent taking into account the dispersion associated to each measurement. This suggests that effective long term stabilization was achieved by GA on magnetic nanoparticles. On the other hand, GA-Mag-b displayed lower stability in terms of Dhs values in water media as it can be seen in Fig. 7b ii). A decrease around 50% with respect to the initial hydrodynamic average value was observed measuring during the assayed period of time. Although other researchers have found similar results, it is important to mention that in most of the examples found in the literature a coupling agent was required to achieve these kinds of properties on GA coated nanoparticles [17,18], but in our work none crosslinking agent was further employed.

3.3. Possible mechanism of formation: difference between two explored routes

Based on the characterization data of GA-Mag nanoparticles obtained by the two explored synthesis routes, it is feasible to predict a possible mechanism for the formation of these materials. As it was earlier commented, GA chemical structure presents a major polysaccharide and a minor glycoprotein fraction. Hence, in general terms, the kinds

of interactions expected to occur between the polysaccharide and iron oxide nucleus are: i) electrostatic and/or ii) hydrophobic ones. Besides, another possibility is the complex formation, giving by the biopolymer bridging to magnetite nucleus. These three types of linkage of the biopolymer to the magnetic cores are supported by some of the characterization data earlier supplied.

In the initial stages of the synthesis, the pH of the media is highly acidic (approx. 2) due to the mixed Fe^{2+}/Fe^{3+} solution in contact with polymeric moieties. The addition of the NH_4OH solution gradually raises the pH with the consequent formation of the first magnetite nucleus. In such conditions, magnetite and GA exhibit opposite surface charge, as it is revealed by data of ζ (see Fig. 5). Then electrostatic interactions are highly possible to occur, in agree with other author's findings [13,22]. Own FTIR data (see Fig. 1b) also support the proposed mechanism, confirming the interactions between GA and iron oxide groups. This is evident from the shift of the band located at around $3400 \ cm^{-1}$ observed in GA-Mag with respect to the broad band present in raw GA spectrum. These observations, together with data from the available literature [15,19], confirm the occurrence of interactions through hydrogen bonding, between carboxylic groups of gum Arabic and hydroxyl groups of magnetite. These electrostatic interactions could be attributable to a bridge formed between two functional groups during the co-precipitation.

At pH higher than the pH_{PZC} of magnetite (>7.1), both, polymer and iron oxide, have negative surface charge. Therefore, steric interactions could be the responsible for the GA binding at these stages of the synthesis procedure. In this work's case the steric interactions is believe that play a key role in order to justify the stabilization mechanism of

magnetic nanoparticles by the polymeric moieties. The hydrophilic nature of GA-Mag is only explained considering that the GA chains bind to iron oxide in such a way in that charged (mainly negative) functional groups remained surface exposed, performing electrostatic repulsion between nanoparticles. This fact only may take place if not all the functional groups of the biopolymer are interacting with iron oxide surface groups [14,16,36].

On the other hand, the magnetic nucleus in formation as well as the Fe precursors in solution could achieve coordination complexes, of different chemical structures, from their interaction with the amine and/or carboxylic groups of the glycoprotein fraction of the polymer [8,37].

4. Potential applications in hyperthermia treatments

To characterize the potential of our formulations for magnetic hyperthermia, the SAR of GA-Mag-b colloid was measured against field amplitude at a constant frequency of 260 kHz (Fig. 8a) and against frequency at constant field amplitude of 17.4 kA/m (Fig. 8b). In Fig. 8a linear behavior is observed for H_0 lower than 12 kA/m. This finding is in agreement with a theoretical model proposed by Rosensweig [38]. Using higher field amplitudes, the SAR field dependence departs from linearity and tends to saturation. Theoretically, SAR is proportional to the area enclosed by the dynamic magnetization cycle, in this way, when the applied field is large enough to saturate the sample, the maximum coercive field equals anisotropy field and SAR no longer increases. This may explain the behavior experimentally observed. On the other hand, it can be observed that SAR monotonously increases with frequency. Single-domain magnetic NPs are known to dissipate heat through Néel and Brown magnetic relaxation processes with a relaxation time $\tau = (\tau_N^{-1} + \tau_B^{-1})^{-1}$. Néel and Brown relaxation times are $\tau_N = \tau_0 e^{KV/k_BT}$ and $\tau_B = 3\eta V_H/k_BT$ respectively. In the framework of linear response theory SAR can be modeled as $SAR_t = \frac{\mu_0^2 \pi \rho H_0^2 M_s^2 V}{3k_BT} \frac{2\pi f^2 \tau}{1+(2\pi f \tau)^2}$.

The SAR vs. H_0^2 and SAR vs. f measurements were well fitted with previous equation using anisotropy constant K as fitting parameter. Resulting in 36.3 kJ/m^3 and 37.2 kJ/m^3 for field and frequency dependence respectively. Using K = 36.3 kJ/m^3 and structural and magnetic measured properties SAR$_t$ was simulated restricting field parameters intervals to the accepted biomedical window. As can be observer in Fig. 8a, linearity holds up to 12 kA/m, defining the validity range of linear response. Simulation is shown in Fig. 8c. The best value satisfying both conditions appears at 12 kA/m and 417 kHz corresponding 74 W/g. In the figure, the projection delimits the SAR within the biomedical window.

Largest SAR of 218 W/g$_{Fe}$ was measured out of the discussed condition at 260 kHz and field amplitude of 52 kA/m (Fig. 8c). The biomedical window for RF applications resulted from one experiment reporting that parts of the human body with a mean diameter of 0.3 m cannot be exposed without discomfort to RF fields for which the product fH_0 is larger than 5 10^9 A/ms [30]. However, it has been pointed out that there is a need for new independent determinations of the discomfort factor and also for a general discussion on its definition [39].

5. Concluding remarks

Highly versatile novel gum Arabic/Fe$_3$O$_4$ nanoparticles have been fabricated using a simple, non-time consuming and inexpensive method.

After an exhaustive characterization, it was found that hybrid nanomaterials having improved and specific properties (such as size, superparamagnetism and surface charge) with respect to the raw materials were obtained. Especially their hydrophilic nature enables to form highly stable colloidal suspensions in water. In fact they were able to, maintain their Dh for more than one month. The GA-Mag nanoparticles sizes ranged from 70 to 80 nm, while the sizes of magnetic core were lower than 20 nm. The aggregation state of the polymer during
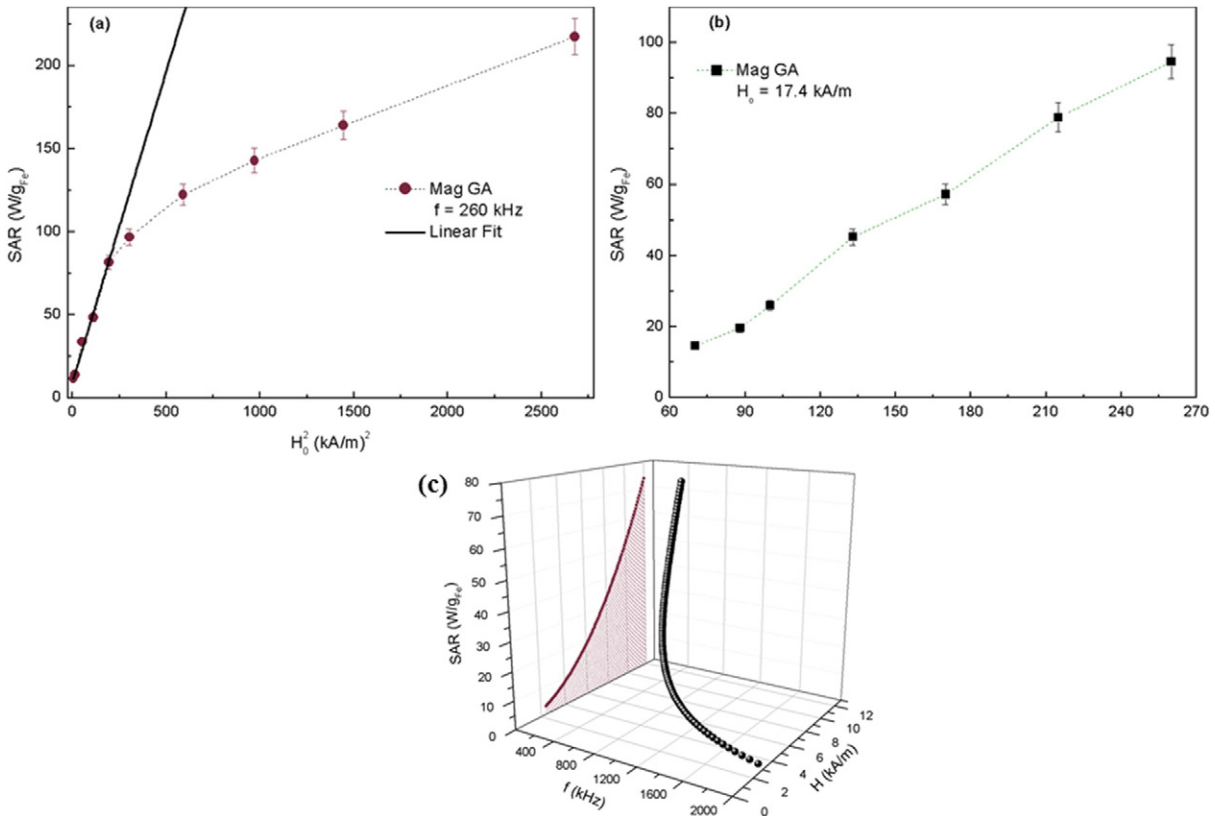

Fig. 8. (a) SAR of GA-Mag-b colloid was measured against field amplitude at a constant frequency of 260 kHz and (b) against frequency at constant field amplitude of 17.4 kA/m (c) SAR Simulation and projection within the biomedical window.

synthesis (solid or in solution) seems not to have an important impact on the properties of obtained nanoparticles. A slight difference was related to greater stability of GA-Mag-a in aqueous dispersion when compared with GA-Mag-b. Another more marked difference was given by the proportion of GA linked to the MNPs surface. According to TGA data, GA-Mag-a is composed for already 39% of GA whereas GA-Mag-b has about 22% in weight.

Properties such as size, polydispersity and stability in aqueous colloidal suspensions turned these MNPs efficient tool to hyperthermia treatments. Restricting field values to linear response theory and to the accepted biomedical window, maximum useful predicted value is 74 w/g Fe at 417 kHz and 12 kA/m. Leaving this restrictions SAR values of 218 W/g_{Fe} was measured at 52 kA/m and 260 kHz.

Acknowledgments

References

[1] S.C.N. Tang, I.M.C. Lo, Magnetic nanoparticles: essential factors for sustainable environmental applications, Water Res. 47 (2013) 2613–2632, http://dx.doi.org/10.1016/j.watres.2013.02.039.

[2] D.L. Zhao, X.X. Wang, X.W. Zeng, Q.S. Xia, J.T. Tang, Preparation and inductive heating property of Fe3O4-chitosan composite nanoparticles in an AC magnetic field for localized hyperthermia, J. Alloys Compd. 477 (2009) 739–743, http://dx.doi.org/10.1016/j.jallcom.2008.10.104.

[3] S.L. Saville, B. Qi, J. Baker, R. Stone, R.E. Camley, K.L. Livesey, L. Ye, T.M. Crawford, O. Thompson Mefford, The formation of linear aggregates in magnetic hyperthermia: implications on specific absorption rate and magnetic anisotropy, J. Colloid Interface Sci. 424 (2014) 141–151, http://dx.doi.org/10.1016/j.jcis.2014.03.007.

[4] A.M.G.C. Dias, A. Hussain, A.S. Marcos, A.C.A. Roque, A biotechnological perspective on the application of iron oxide magnetic colloids modified with polysaccharides, Biotechnol. Adv. 29 (2011) 142–155, http://dx.doi.org/10.1016/j.biotechadv.2010.10.003.

[5] A.K. Gupta, M. Gupta, Synthesis and surface engineering of iron oxide nanoparticles for biomedical applications, Biomaterials 26 (2005) 3995–4021, http://dx.doi.org/10.1016/j.biomaterials.2004.10.012.

[6] P. Nicolás, M. Saleta, H. Troiani, R. Zysler, V. Lassalle, M.L. Ferreira, Preparation of iron oxide nanoparticles stabilized with biomolecules: experimental and mechanistic issues, Acta Biomater. 9 (2013) 4754–4762, http://dx.doi.org/10.1016/j.actbio.2012.09.040.

[7] D. Hritcu, G. Dodi, M. Silion, N. Popa, M.I. Popa, Composite magnetic chitosan microspheres: in situ preparation and characterization, Polym. Bull. 67 (2011) 177–186, http://dx.doi.org/10.1007/s00289-010-0439-y.

[8] V.L. Lassalle, R.D. Zysler, M.L. Ferreira, Novel and facile synthesis of magnetic composites by a modified co-precipitation method, Mater. Chem. Phys. 130 (2011) 624–634, http://dx.doi.org/10.1016/j.matchemphys.2011.07.035.

[9] J.-L. Bridot, A.-C. Faure, S. Laurent, C. Rivière, C. Billotey, B. Hiba, M. Janier, R.J. Vé, J.-L. Coll, L. Vander Elst, R. Muller, S. Phane Roux, P. Perriat, O. Tillement, Hybrid Gadolinium Oxide Nanoparticles: Multimodal Contrast Agents for in Vivo Imaging, 2007 5076–5084, http://dx.doi.org/10.1021/ja068356j.

[10] F.A. Dendrimers, K.J. Landmark, S. Dimaggio, J. Ward, Ḱ.C. Kelly, S. Vogt, S. Hong, A. Kotlyar, A. Myc, T.P. Thomas, J.E. Penner-hahn, J.R. Baker, M.M.B. Holl, B.G. Orr, Testing of Superparamagnetic Iron Oxide Nanoparticles Targeted Using, 2, 2008 773–783.

[11] J. Shin, R.M. Anisur, M.K. Ko, G.H. Im, J.H. Lee, I.S. Lee, Hollow manganese oxide nanoparticles as multifunctional agents for magnetic resonance imaging and drug delivery, Angew. Chem. Int. Ed. 48 (2009) 321–324, http://dx.doi.org/10.1002/anie.200802323.

[12] R. Dror, Yael, Cohen, Yachin, Yerushalmi-Rozen, Structure of Gum Arabic in aqueous solution, J. Polym. Sci. Part B Polym. Phys. 44 (2006) 3265–3271.

[13] O.C. Wilson, E. Blair, S. Kennedy, G. Rivera, P. Mehl, Surface modification of magnetic nanoparticles with oleylamine and gum Arabic, Mater. Sci. Eng. C 28 (2008) 438–442, http://dx.doi.org/10.1016/j.msec.2007.04.008.

[14] A.C.A. Roque, A. Bicho, I.L. Batalha, A.S. Cardoso, A. Hussain, Biocompatible and bioactive gum Arabic coated iron oxide magnetic nanoparticles, J. Biotechnol. 144 (2009) 313–320, http://dx.doi.org/10.1016/j.jbiotec.2009.08.020.

[15] S.S. Banerjee, D.H. Chen, Fast removal of copper ions by gum Arabic modified magnetic nano-adsorbent, J. Hazard. Mater. 147 (2007) 792–799, http://dx.doi.org/10.1016/j.jhazmat.2007.01.079.

[16] D.N. Williams, K.A. Gold, T.R.P. Holoman, S.H. Ehrman, O.C. Wilson, Surface modification of magnetic nanoparticles using gum Arabic, J. Nanopart. Res. 8 (2006) 749–753, http://dx.doi.org/10.1007/s11051-006-9084-7.

[17] A. Bicho, A.C.A. Roque, A.S. Cardoso, P. Domingos, Í.L. Batalha, In vitro studies with mammalian cell lines and gum arabic-coated magnetic nanoparticles, J. Mol. Recognit. 23 (2010) 536–542, http://dx.doi.org/10.1002/jmr.1066.

[18] L. Zhang, F. Yu, A.J. Cole, B. Chertok, A.E. David, J. Wang, V.C. Yang, Gum Arabic-coated magnetic nanoparticles for potential application in simultaneous magnetic targeting and tumor imaging, AAPS J. 11 (2009) 693–699, http://dx.doi.org/10.1208/s12248-009-9151-y.

[19] S.S. Banerjee, D.H. Chen, Glucose-grafted gum Arabic modified magnetic nanoparticles: preparation and specific interaction with Concanavalin A, Chem. Mater. 19 (2007) 3667–3672, http://dx.doi.org/10.1021/cm070461k.

[20] I. Mahmood, I. Ahmad, G. Chen, L. Huizhou, A surfactant-coated lipase immobilized in magnetic nanoparticles for multicycle ethyl isovalerate enzymatic production, Biochem. Eng. J. 73 (2013) 72–79, http://dx.doi.org/10.1016/j.bej.2013.01.017.

[21] S.S. Banerjee, D.H. Chen, Grafting of 2-hydroxypropyl-β-cyclodextrin on gum Arabic-modified iron oxide nanoparticles as a magnetic carrier for targeted delivery of hydrophobic anticancer drug, Int. J. Appl. Ceram. Technol. 7 (2010) 111–118, http://dx.doi.org/10.1111/j.1744-7402.2008.02332.x.

[22] A.C.A. Roque, O.C. Wilson, Adsorption of gum Arabic on bioceramic nanoparticles, Mater. Sci. Eng. C 28 (2008) 443–447, http://dx.doi.org/10.1016/j.msec.2007.04.009.

[23] S. Bhattacharya, A. Roychowdhury, V. Tiwari, A. Prasad, R.S. Ningthoujam, A.B. Patel, D. Das, S. Nayar, Effect of biomimetic templates on the magneto-structural properties of Fe3O4 nanoparticles, RSC Adv. 5 (2015) 13777–13786, http://dx.doi.org/10.1039/C5RA00705D.

[24] D.T. Nguyen, K. Kim, Controlled synthesis of monodisperse magnetite nanoparticles for hyperthermia-based treatments, Powder Technol. 301 (2016) 1112–1118, http://dx.doi.org/10.1016/j.powtec.2016.07.052.

[25] E.C. Rodrigues, M.A. Morales, S.N. de Medeiros, N.M. Suguihiro, E.M. Baggio-Saitovitch, Pluronic® coated sterically stabilized magnetite nanoparticles for hyperthermia applications, J. Magn. Magn. Mater. 416 (2016) 434–440, http://dx.doi.org/10.1016/j.jmmm.2016.05.033.

[26] S. Sarkar, E. Guibal, F. Quignard, A.K. SenGupta, Polymer-supported metals and metal oxide nanoparticles: synthesis, characterization, and applications, J. Nanopart. Res. 14 (2012) http://dx.doi.org/10.1007/s11051-011-0715-2.

[27] J.O. Kim, T. Ramasamy, T.H. Tran, J.Y. Choi, H.J. Cho, J.H. Kim, C.S. Yong, H.G. Choi, Layer-by-layer coated lipid-polymer hybrid nanoparticles designed for use in anticancer drug delivery, Carbohydr. Polym. 102 (2014) 653–661, http://dx.doi.org/10.1016/j.carbpol.2013.11.009.

[28] I. Hilger, In vivo applications of magnetic nanoparticle hyperthermia, Int. J. Hyperth. 29 (2013) 1464–5157, http://dx.doi.org/10.3109/02656736.2013.832815.

[29] D.F. Coral, P. Mendoza Zalis, M.E. De Sousa, D. Muraca, V. Lassalle, P. Nicolas, M.L. Ferreira, M.B. Fernandez Van Raap, Quasi-static magnetic measurements to predict specific absorption rates in magnetic fluid hyperthermia experiments, J. Appl. Phys. 115 (2014) http://dx.doi.org/10.1063/1.4862647.

[30] S.I.C.J. Palma, A. Carvalho, J. Silva, P. Martins, M. Marciello, A.R. Fernandes, P. Morales, A.C.A. Roque, Covalent Coupling of Gum Arabic Onto Superparamagnetic Iron Oxide Nanoparticles for MRI Cell Labeling: Physicochemical and In Vitro Characterization, 2015 http://dx.doi.org/10.1002/cmmi.1635.

[31] L.J.E.V. Groman, E.T. Menz, P.M. Enriquez, C. Jung, J.M. Lewis, Delivery of Therapeutic Agents to Receptors Using Polysaccharides, 1994.

[32] R.M.C.U. Schwertmann, Iron Oxides in the Laboratory: Preparation and Characterization, second ed. Wiley-VCH, 2000.

[33] H. Mallik, N. Gupta, A. Sarkar, Anisotropic electrical conduction in gum arabica-a biopolymer, Mater. Sci. Eng. C 20 (2002) 215–218, http://dx.doi.org/10.1016/S0928-4931(02)00036-X.

[34] M.J. Zohuriaan, F. Shokrolahi, Thermal studies on natural and modified gums, Polym. Test. 23 (2004) 575–579, http://dx.doi.org/10.1016/j.polymertesting.2003.11.001.

[35] L.S. Jeremy Mark Berg, J.L. Tymoczko, Biochemistry, Freeman W. H., 2012

[36] C. Sanchez, D. Renard, P. Robert, C. Schmitt, J. Lefebvre, Structure and rheological properties of acacia gum dispersions, Food Hydrocoll. 16 (2002) 257–267, http://dx.doi.org/10.1016/S0268-005X(01)00096-0.

[37] Y.K. Leong, U. Seah, S.Y. Chu, B.C. Ong, Effects of gum Arabic macromolecules on surface forces in oxide dispersions, Colloids Surf. A Physicochem. Eng. Asp. 182 (2001) 263–268, http://dx.doi.org/10.1016/S0927-7757(00)00826-8.

[38] R.E.E. Rosensweig, Heating magnetic fluid with alternating magnetic field, J. Magn. Magn. Mater. 252 (2002) 370–374, http://dx.doi.org/10.1016/S0304-8853(02)00706-0.

[39] P.M. Zélis, G.A. Pasquevich, S.J. Stewart, M.B.F. Van Raap, J. Aphesteguy, I.J. Bruvera, C. Laborde, B. Pianciola, S. Jacobo, F.H. Sánchez, Structural and magnetic study of zinc-doped magnetite nanoparticles and ferrofluids for hyperthermia applications, J. Phys. D. Appl. Phys. 46 (2013) 125006, http://dx.doi.org/10.1088/0022-3727/46/12/125006.